The Astrophysical Journal, 606:466–482, 2004 May 1

CORONAL VARIABILITY IN THE YOUNG CLUSTER NGC 2516

S. J. Wolk, F. R. Harnden, Jr., S. S. Murray, and N. R. Adams
Harvard-Smithsonian Center for Astrophysics, 60 Garden Street, Cambridge, MA 02138

F. Damiani, E. Flaccomio, G. Micela, and S. Sciortino
INAF-Osservatorio Astronomico di Palermo G. S. Vaiana, Piazza del Parlamento 1, I-90134 Palermo, Italy

and

R. D. Jeffries
Department of Physics, Keele University, Keele, Staffordshire ST5 5BG, UK
Received 2003 July 1; accepted 2004 January 13

ABSTRACT

NGC 2516 has been observed by *Chandra* several times in order to correct the plate scale of the spacecraft's focal plane instruments. Because of this, *Chandra* has observed NGC 2516 with all four imaging arrangements available. In addition, NGC 2516 has been observed as part of the High Resolution Camera (HRC) guaranteed time program and is scheduled for return plate scale calibration visits. This makes it the best cluster to study for long-term variability. NGC 2516 is about 140 Myr old and less than 400 pc away. In our first paper, we discussed the detection of 150 X-ray sources (42% of which are identified as cluster members) in the calibration data taken during the orbital activation phase of the *Chandra* mission. In our second paper, we combined all the extant data sets and detected 284 sources, more than half of which are considered likely cluster members. In this our third paper, we further explore techniques of combining Advanced CCD Imaging Spectrometer (ACIS) and HRC *Chandra* data for timing analysis. We have been able to combine almost 70 ks of observation time, spread over five epochs, to study variability in this cluster on multiple timescales. We find that while stochastic variability rates are about the same for all objects in the sample, the timescale for detecting variability is shorter for late-type stars. Both stochastic and flare variability rates seen in NGC 2516 are similar to those seen in younger clusters IC 348, NGC 1333, and M42.

Subject headings: open clusters and associations: individual (NGC 2516) — stars: coronae — X-rays: stars

1. INTRODUCTION

From the earliest *Einstein* observations, it has been clear that young stars, both pre–main sequence (PMS) and zero-age main sequence (ZAMS), are bright, time-variable X-ray sources (Feigelson & Decampli 1981; Montmerle et al. 1983). The source of the X-ray emission has been assigned to various physical mechanisms depending on the mass of the star. These include (from high to low mass) wind–interstellar medium interactions, emission of an unseen companion, an α-Ω dynamo driven by the differential rotational shearing of the stellar core with convective envelope, as well as an α-α or turbulent dynamo capable of producing X-ray emission without core-envelope shearing.

Variability studies allow us to begin to assess the plausibility of these mechanisms. X-ray generation mechanisms can be constrained by the timescales and flux changes observed in the variability. The key to understanding the root cause of X-ray emission in young stars is to create data sets of similar stars and study how observables such as luminosity, temperature, and variability change with the key physical parameters of mass and age.

Marino, Micela, & Peres (2000) and Marino et al. (2002) have studied the variability of nearby normal dG–dM stars and found that they are nonvariable on timescales of hours. However, many of these stars do show variations when flux levels are compared among observations separated by months. Stelzer, Neuhäuser, & Hambaryan (2000) analyzed *ROSAT* archival data of PMS stars in Taurus-Auriga-Perseus and found the X-ray flare rate may depend on multiplicity, stellar age, and rotation rate. They find that multiple stars, younger stars, and faster rotators tend to show more flares. Thus, X-ray variability may be useful as a diagnostic of stellar activity and for validation of the existing models.

NGC 2516 is a southern open cluster that has been intensively studied in X-rays. Sometimes referred to as the "Southern Pleiades," NGC 2516 is about 140 Myr old (Meynet, Mermilliod, & Maeder 1993) and less than 400 pc away (390 pc; Jeffries, Thurston, & Pye 1997). It occupies an interesting place in the evolutionary time sequence, somewhat older than the Pleiades, yet younger than the Hyades. NGC 2516 is also somewhat more compact than these clusters. NGC 2516 efficiently gives us a rich and homogeneous sample to study variability in young main-sequence stars with same age, distance, and composition.

NGC 2516 is a unique cluster because it is being observed by both *Chandra* and *XMM-Newton* (Sciortino et al. 2001; Ramsay, Harra, & Kay 2003) to measure the plate scale spacecrafts' focal plane instruments. Because of this, *Chandra* observed NGC 2516 with all four imaging arrangements available. In addition, it has been observed as part of the High Resolution Camera (HRC) guaranteed time program and *Chandra* has made return calibration visits. In all, there have been eight successful observations of NGC 2516 by *Chandra* spaced over about 19 months (see Damiani et al. 2003 [hereafter Paper II], Table 1). This makes it the best cluster to date to study for long-term variability.

In our first *Chandra*-based study of this cluster (Harnden et al. 2001, hereafter Paper I), we examined only the calibration data for the HRC-I and Advanced CCD Imaging Spectrometer (ACIS-I) detectors. We detected about 150 sources, 42% of which have been confirmed as cluster members.

G and K stars in NGC 2516 were found to be less X-ray–luminous than the G and K Pleiades stars, while the median $\log L_{\rm X}$ value for NGC 2516 F-type stars is higher than that of the Pleiades. Our most recent study (Paper II) reaches luminosities of $\log L_{\rm X} = 28.69$ ergs s^{-1} through the combined analysis of eight HRC-I, ACIS-I, and ACIS-S data sets. In Paper II, we find a luminosity function for late-type stars that is significantly lower than that of the Pleiades. We also detect almost all the chemically peculiar A stars and find that wide binarity has little impact on X-ray activity.

In this paper, we explore the variability properties of the sources detected in Paper II with the goal of comparing these results with those of other young open clusters investigated by *Chandra*. In § 2, we briefly review the qualities of the NGC 2516 data set. In § 3, we discuss the special difficulties in the creation of light curves used in the analysis. Section 4 defines the terms (e.g., "stochastic variability" and "flare") that are applied to the light curves in § 5. Then we compare our results with those of other clusters as obtained by other groups in § 6.

2. DESCRIPTION OF THE DATA SET

Chandra observations of NGC 2516 performed from 1999 through 2001 form a very heterogeneous data set. This data set is composed of three HRC observations, two ACIS-I observations, and two ACIS-S observations, all made on a common center. An eighth observation, also with ACIS-S3 at the aim point, was made slightly off the field center to improve the boresight solution. In Paper II, we detailed our method of analysis of the eight independent observations. We also discussed our creation of a single data set that combined the HRC-I and ACIS-I observations to form a single deep event list that was used for the deepest possible source search. In the variability analysis presented here, we confined ourselves to sources detected on the sum of these five observations: two observations with ACIS-I separated by about 14 hr and three observations with HRC-I separated from each other by four and 13 months, commencing two months after the ACIS observations. The sources correspond to sources 1 through 206 in Table 3 of Paper II. Optical source identifications are also taken from Paper II. To maximize the uniformity of an awkward data set, we explicitly ignore scores of detected sources seen only on the ACIS-S array, as these have a relatively short amount of total observing time.

Following Paper II, membership and binarity are taken from Jeffries, Thurston, & Hambly (2001) and Jeffries et al. (1997). We determine spectral type following Jeffries et al. (2001) by using $V-I$ color for later type stars (G–M) and identifying earlier stars via $B-V$ color. Extinction was taken from Dach & Kabus (1989) and assumed to be $E(B-V) = 0.12$ and $E(V-I) = 0.1536$. Spectral types were chosen as in Paper II. Colors for the brightest stars were taken from an earlier study of NGC 2516 (Jeffries et al. 1997). By using the summed ACIS-I and HRC-I data in Paper II we have enlarged the sample of detected members from the 82 stars of Paper I to 155 stars. In the current paper, we have 139 X-ray–detected cluster members. This number is somewhat smaller than Paper II because we have excluded data from the ACIS-S observations (observation IDs [ObsIDs] 66 and 1229) and from the nonstandard ACIS observation 1458.

We note the similar X-ray detection rates for all types of stars, with the exception of M stars (Paper II, Table 7). Detection rates for B stars are presumably high because of their winds. F–K stars are presumably detected because of coronal activity derived from a dynamo process. The decreasing detection rate at low mass is consistent with the interpretation that the maximum surface flux is constant; the stars of later spectral types have smaller surface areas and thus are more difficult to detect. The similarity in the detection rate of A stars with that of the other stars is harder to explain. A stars are believed not to have the winds needed to create shock-driven X-rays, and their interiors are thought not to be convective, a precondition for a dynamo. A common supposition is that A stars detected at X-ray energies are part of binary systems, but Table 7 of Paper II shows that the X-ray detection rate of A stars is nearly identical to that of K stars. Thus, if this supposition were to be true, on average, each A star would have a K star companion. While this seems unlikely, Jeffries et al. (1997) noted that NGC 2516 has a large number of magnetic A stars. Perhaps these stars have a greater tendency toward low-mass companions or perhaps the existence of a low-mass companion caused the observed magnetic anomaly.

Of the 206 X-ray sources considered here, 67 (33%) were not identified with optical cluster members. Of these, 24 are identified with sources in the Jeffries et al. catalogs, which are explicitly found not to be cluster members. Most of these appear to be background stars; about half are quite red, so they are possible dMe stars. One X-ray source has colors consistent with those of a white dwarf. The remaining 43, 21% of the total of the X-ray sources, are nominally unknown, since they were photometrically undetected in a survey that was complete past $V = 20$. As discussed in Paper II, the unidentified sources are possibly extragalactic sources. At our sensitivities, the resulting $F_{\rm X}/F_v$ ratios are too high to be of stellar nature. Of course, some of the photometrically detected X-ray sources, which are not cluster members, may also be active galactic nuclei (AGNs) as well. In addition, some of the optically faint X-ray sources could be neutron stars or distant low-mass X-ray binaries.

3. CREATION OF LIGHT CURVES

We discovered almost immediately that the background was highly variable in two of the observations (HRC ObsID 27 and ACIS ObsID 1232). In the case of the ACIS data, this occurred because they were taken during the first month of the mission. The ACIS detectors were operated while the spacecraft was still relatively close to the Earth during the early mission. The local background due to trapped high-energy particles is quite high and nonuniform at these low altitudes. The first half of ObsID 27 was subject to a large background radiation event. Given a constant background, it is straightforward to create a light curve by extracting the photon arrival times within a given aperture using simple tools and subtract off an area-scaled background. Temporal background variations require a more sophisticated technique. We settled on functionality in the CIAO version 2.2 tool DMEXTRACT. Using DMEXTRACT, we created a time histogram of the photon arrival times within a given source region. We simultaneously subtract the counts observed in an appropriately normalized background region.

For the background region we created a "Swiss cheese" background image by removing all the sources detected in each observation using DMCOPY. We chose an aperture of 3 times the radius determined by the PWDetect (F. Damiani et al. 2004, in preparation)[1] algorithm. This enlarged aperture

[1] See also http://www.astropa.unipa.it/progetti_ricerca/PWDetect.

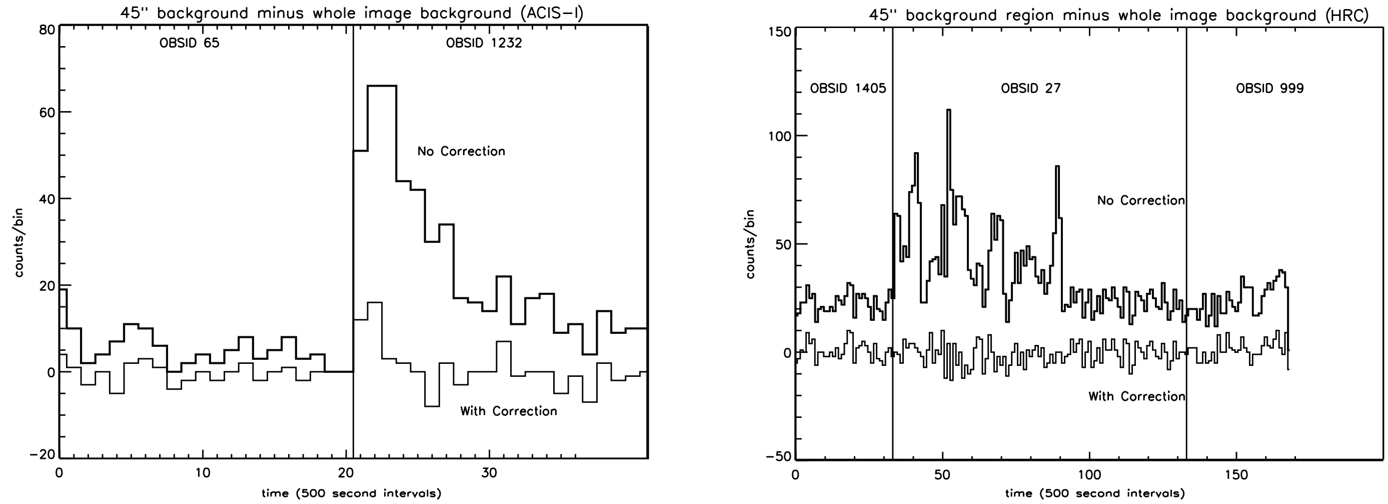

Fig. 1.—Test of the effectiveness of our background subtraction for both ACIS (*left*) and HRC (*right*). The upper curve represents the count rate in a 45″ diameter region. The lower curve is the result of subtracting a scaled Swiss cheese background from the background region. Temporal effects cancel well. HRC and ACIS-I residuals are less than 2×10^{-4}counts arcsec^{-2} per 500 s time bin. Poissonian errors are valid.

should have included over 90% of the energy from each source. Background maps were made for each of the HRC exposures and for each of the ACIS-I observations.[2]

We chose a time bin of 500 s per bin as a compromise between having good signal per bin for most of the bright sources and having sufficient temporal resolution to detect flares of about 2000 s in length. To verify the validity of the background extraction, a 45″ radius region devoid of sources and located near the aim point was selected as a background comparison region. As shown in Figure 1, the background correction *appears* to work quite well. However, periods of very high noise in off-axis source are still detectable.

The residuals in the ACIS-I and HRC-I image had an absolute value of less than 0.3 counts per 500 s in a 45″ diameter aperture. In a more typical 3″ aperture, the residual is less than 0.002 counts per 500 s bin.

Despite the general effectiveness of this approach, tests performed using simulated constant sources showed variability. This was due to the dramatic background variations at the beginning of the ACIS observations as well as the first half of the long HRC observation (ObsID 27). The light curves were therefore trimmed to remove the time periods contaminated by high background that, while subjectively determined, were periods during which the mean signal was higher than the nominal mean signal by more than 3 σ. The final usable durations are 9.5 ks for ACIS-I ObsID 65, 7.0 ks for ACIS-I ObsID 1232, 17 ks for HRC-I ObsID 1405, 21.5 ks for HRC-I ObsID 27 and 17.5 ks for HRC-I ObsID 999. This is a more conservative time filtering (i.e., results in shorter usable exposures) than that applied to the same data sets for pure source-detection purposes (cf. Paper II, Table 3).

DMEXTRACT was run separately for each source and each ObsID, with the appropriate background. Data were first trimmed to reduce the noise. In the case of HRC, we selected photons in the pulse height amplitude range between 35 and 254 as only non–X-ray events lay outside that range. Similarly, for the ACIS data, only energies between 300 eV and 8 keV having grades 0, 2, 3, 4, or 6 were accepted for analysis. To choose extraction regions we followed Paper II and used extraction regions 3 times the radius of the 50% encircled energy radius for that off-axis position. This assures inclusion of at least 95% of the energy from each source.[3] Data were binned to produce net counts per 500 s. The extractions from like detectors were pruned by removing the bins contaminated by highly variable background in such a way as to guarantee a full 500 s low noise observation was represented in each bin. The data produced for analysis were bin_number, bin_start, bin_stop, and net_counts per bin. The result was 412 light curves, 206 for 56 ks of HRC-I, and 206 for 16.5 ks of ACIS-I. However, some of the ACIS-I light curves are blank, as the source is located off of the detector.

4. VARIABILITY ANALYSIS

In some cases, like that of the striking flare shown at the top of Figure 7 in Flaccomio et al. (2003a), the existence and nature of the variability is quite easy to assess. However, most situations are far less clear-cut. We sought a systematic methodology for determining the existence of variability and its nature. We chose to address this quantitatively by answering three questions:

1. Was the flux from the source consistent with the hypothesis of constancy?
2. Did the flux level change among separate observations?
3. Did the source flare?

4.1. *Question 1: Is the Source Constant?*

X-ray variability takes many forms. Sometimes there is a dramatic peak in the flux followed by a return to the original level. More often, however, as demonstrated by these data, the flux shows a steady rise or decline, and sometimes the flux simply varies much more wildly than expected from Poisson statistics. This last case is very hard to quantify and test. We pursued several approaches.

[2] We discovered a feature in the CIAO region library during this process: When many small regions are removed from a large region, the total area as reported by the CIAO data model increases instead of decreasing. The error in the calculated area is on the order of 1% for the HRC data, but may reach 10% in the case of the ACIS data. The nature of the error is such that too little background is subtracted. Background was renormalized to compensate.

[3] *Chandra* Proposers' Observatory Guide, chap. 4.

The one-sample Kolmogorov-Smirnov (K-S) test determines whether the observed population is drawn from a functional form. In the case of a nonvariable object the functional form is linear: a constant photon arrival rate. However, our data were time-binned in order to properly subtract out times of high background. To simulate the effective photon arrival times, the events in each bin were "spread out" throughout the bin as though they had arrived uniformly within the bin. For example, if a bin had four events, they were assigned times of bin_start + (1/8)*500, bin_start + (3/8)*500, bin_start + (5/8)*500, and bin_start + (7/8)*500, respectively. Of course, this is an approximation to the actual photon arrival times and should result in a systematically higher probability of finding a light curve compatible with being constant and prevents us from detecting any variation on timescales smaller than the 500 s bin size.

One could directly test the time histogram using a two-sample K-S test. A two-sample K-S test examines whether the observed population can be derived from the hypothesized population. In the case of these light curves, the simple nonvariable object hypothesis is that the count rate per 500 s bin is a Poisson distribution about a mean. Here the Poisson distribution mean is the same as the mean of the light curve. We improved this hypothesis by modeling the observed light curve as the result of constant source+Poisson noise sitting on a constant background+Poisson noise—a constant background. The background is scaled for the aperture.

We tested the sensitivity of the K-S test to total counts. We created synthetic variable sources by creating sinusoidal light curves with noise. The light curves had 1, 2, and 3 σ peak-to-peak fluctuations relative to the noise. To fill out the sample space, we also used the observed light curves from 15 very bright sources with counts totals exceeding 200 and with probabilities of being nonconstant of over 99%. We then created 100 simulated light curves derived from the observed light curves from each source for a range of total counts between 15 and 200. At 200 counts, all input sources were detected as nonconstant. The percentage of sources detected at nonconstant dropped nearly linearly from 90% at 160 counts to 43% at 25 counts. Above 160 counts the nonconstant detection rate moved asymptotically to 100%. Below 25 counts, the nonconstant detection rate dropped precipitously at this point, down to 35% at 20 counts.

Simulations were categorized into three groups: "faint" sources too faint to be tested with statistical reliability (these had <25 counts in the two combined ACIS observations or <25 counts in the three combined HRC observations), "moderate" sources with sufficient counts for the statistical tests to give reliable results (>25 total counts but <2 counts ks^{-1}) but were not as luminous as the "bright" sources, which could be used for flux-limited comparison (brighter than 2 counts ks^{-1}). These categories were then used to sort the observed data. We note that data from the ACIS lack a large number of moderate sources. This is because the combined ACIS observing time is short, less than 17 ks; thus, 2 counts ks^{-1} is less than 50% greater than the 25 counts required for statistical significance, leaving a small luminosity window for the moderate sources.

By using the K-S test, there are no "confirmed" variable sources, only highly likely variables. Because of this, we needed to designate an arbitrary acceptable false alarm probability. We conducted one- and two-sample K-S tests against each moderate and bright source detected by each single instrument configuration (not from observations taken with different instruments). All sources found to be nonconstant with $\geq$99% confidence were flagged as stochastically variable sources. In all cases, the one-sample K-S test detected fewer variable sources than the two-sample K-S test. Since the one-sample test seemed more conservative, we chose it as our primary test of stochastic variability.

4.2. *Question 2: Does the Source Quiescent Level Change?*

Not all variability is completely random. A unique feature of this data set with respect to other *Chandra* data sets of young clusters is the number of visits. Each visit was at least 7 ks, so there are good statistics for many of the sources. Unfortunately, the count rate among the different detectors cannot easily be compared because the rate depends on the effective area, which in turn depends on the source energies.

We therefore chose to compare count rates *only among observations made with like detectors*. The two ACIS observations were separated by one orbit; thus, the affect on the gain variation by radiation damage that occurred during the first weeks of the mission was minimal. HRC showed little gain variation over the first 2 yr of the *Chandra* mission.

We defined a quiescent level "shift" to be a change in the mean flux among observations with the same detector, such that the mean flux differs by more than 2.5 σ. This definition gives us confidence that only true quiescent level changes are detected. However, since 1 σ represents a smaller fraction of the total signal of a bright source than a faint source, it is easier to detect smaller fractional changes in the quiescent level of a bright source. We used data from Paper II, excluding sources on the backside-illuminated CCDs and sources above 206 in Table 3. Backside-illuminated CCDs were excluded because the background properties of these detectors are dramatically different from those of the HRC-I or front-illuminated CCDs.

4.3. *Question 3: Does the Source Flare?*

The most common form of X-ray variability discussed in the literature is flaring. In these cases, well documented in *Einstein*, *ROSAT*, *EXOSAT*, and *ASCA* data, the flux from a star rapidly increases from a quiescent level to a sharp peak. The flux then quickly drops in a quasi-exponential decay. The low Earth orbit observing windows of previous X-ray satellites usually limited observations to the detection of either the rise or the fall of a flare, but not both. In contrast, entire flares are routinely observed using *Chandra* or *XMM-Newton* because of their long-period highly elliptical orbits. Our usage of the one-sample K-S test to detect variability is similar to that used by Getman et al. (2002) in their analysis of NGC 1333, but with a very important difference. Getman et al. consider the opposite of "constant" to be "flaring," a characterization with which we disagree. We find many stars with 99% confidence of having nonconstant photon arrival intervals (or 99.5% the value used by Getman et al.) to be nonconstant *without* seeing the traditional flare profile in the light curve. As the term "flare" implies a singular event, we search for flares within our data adopting the technique of Stelzer et al. (2000). We define σ to be the square root of the mean number of counts per 500 s time bin. We then looked at all "moderate" and "bright" sources for periods in which data from three successive bins (25 minutes) exceeded the mean flux by more than 5 σ. In the Sun, most of the flares have characteristic timescales smaller than 25 minutes (see, e.g., Garcia 2000). The relatively poor statistics of the data force a flare definition that excludes these solar-like flares.

We also conducted searches for smaller flares with the excess flux parameter set to 3 σ. This found features in two of the light curves that, upon inspection, are best described as "possible flares." For the remainder of the paper we use a sustained 5 σ deviation from the mean as the definition of a flare.

This approach to defining a flare has an interesting impact on the detection of long-duration flares. In some cases, a flare is occurring throughout an observation period, and examination of data from that period alone reveals no flare. It is only from the inclusion of multiple observations that the flare is detected. This is not a case in which the increase of the observing windows allowed us to detect a flare by increasing the window of opportunity. Instead, the increased duration of the observation window allows us to ascertain, by comparison, that the star was in a flare state.

5. RESULTS

The results of the light curve analysis are given in Table 1 and summarized in Figure 2. The total number of sources in the analysis that achieve our X-ray brightness criteria is 103. Figure 2 shows an annotated color-magnitude diagram of the stars in this study adapted from Table 4 of Paper II. The figure shows variable X-ray sources are found throughout the diagram. Flaring sources are also found throughout the diagram, although three of the flaring sources are found among the 10 reddest objects.

Table 1 is sorted by increasing color index, as given in Paper II, with blue stars at the top. We excluded sources that had less than 25 total counts on either single detector. Nonmember sources and X-ray sources with no optical counterpart are listed at the end. The table has subheadings listing the spectral type, as derived from Table 7 of Paper II. The first column is the source number from Paper II for cross-referencing purposes. Right ascension and declination are in J2000.0. The variability results (none, stochastic, quiescent level change, or flare) are tabulated separately for HRC and ACIS. The "brightness" column characterizes the flux of the sources. "Faint" indicates that the flux is below the 25 count threshold required for reliable results from the K-S test. The notation "moderate" indicates that the flux is above the 25 total count threshold but below 2 counts ks^{-1}, which is defined as "bright." Additional comments in the ACIS brightness column include "off-chip," meaning the source was not on the ACIS array, and "CCD=s3," meaning the source was detected on the backside-illuminated CCD S3 and thus beyond the scope of this paper.

One of our first discoveries is that the three types of flaring described in § 4 are in essence a narrowing of scope. All flaring stars are also detected as quiescent level changes. Most stars with quiescent level changes are variable via the K-S test. If variability is found with greater than 99% confidence but a change in the quiescent level is not seen, then we define this as stochastic variability and "stochastic" appears in the "variability" column. In the case in which the variability found is a change in the quiescent level, "QL" is listed in the "variable" column. In the cases in which the quiescent level shift was not detected as variability by the K-S test, "QL only" is listed. If a flare is detected, then "flare" is noted in place of "QL."

Figures 3, 4, and 5 show interesting yet difficult to assay light curves from stars of several spectral types, as well as X–ray sources that are not cluster members or have no optical counterpart. An examination of the light curves in these figure illustrates the difficulty in quantifying light curves. Only one of the light curves, Src 170 (see Fig. 5), shows a prototypical flare, a rapid rise peaking at more than 100 times the mean flux, followed by an exponential decay. Several stars, including Src 42, Src 169, Src 141, and Src 105, are dominated by flux during one observing window; as the flux during this one window exceeds that in the other windows by more than 5 σ, these are recorded as flares. In most of these cases we seem to have observed the decay of a fairly long-lived (>14 hr) flare.

Although several light curves are consistent with constant emission during one or more observations, all of the light curves shown are considered variable above the 99% confidence level by the one-sided K-S test when the entire duration of all observations in one or the other detectors is taken into account. For example, the HRC portion of Src 25 (Fig. 5) is considered nonvariable (this portion differed from a constant source with *only* 96% probability), even though particular bins deviated from the mean of 0.48 counts per 500 s by over 4.5 counts. However, the distinct brightening seen during the ACIS portion of the observation causes the one-sided K-S test to indicate overall variability at greater than 99% confidence. We do not describe this as a flare because the peak flux sustained over 1500 s was not 5 σ greater than the average of the ACIS flux during that observation. There are many weak features of this nature throughout the data set. Figure 6 shows a selection of nonvariable light curves.

5.1. *Quiescent Level Changes*

Strong distinct changes in quiescent level are rare. Figure 7 shows comparisons among the 378 observation intervals. Nineteen shifts in the mean flux beyond the 3 σ level were detected. We do not consider this behavior to be a priori stochastic, only that a flux was different in one interval relative to others. However, only three of the 19 light curves noted as quiescent level changes are not detected by the K-S test. This happens when the change in flux is too small to be noticed by the K-S test. However, such a change is perceptible when the average flux compared either side of a predetermined location in the light curve (the change in observations). Only one source (source 140) showed quiescent level shifts between both the ACIS observations, separated by about 14 hr, and again between HRC observations, separated by months. Six of the quiescent level changes occurred because of a flare observed during one window, but not the other(s), noted as such in Table 1. The total percentage of observation gaps across which a quiescent level shift was seen and not due to an observed flare was 3.4%.

Of the 29 cluster members detected with ACIS and having over 25 counts, three of them (~10%) showed changes in their quiescent level not attributed to flares. These changes occurred very quickly as the two ACIS observations were separated by a single passage of *Chandra* through the radiation belts. Less than 14 hr elapsed between the last events in the first ACIS observation and the first event of the second ACIS observation. A similar fraction, 7/72, of member stars detected with the HRC showed changes in their quiescent level (independent of flares), despite the fact that the gaps between the HRC observations were much longer—4 and 13 months, respectively.

Thirty percent of the quiescent level changes were detected to occur during the 14 hr which separated the two ACIS observations. This is consistent with the time between observations

TABLE 1

X-Ray Variability Analysis versus Spectral Type

Paper II Source Number	R.A. (J2000.0)	Decl. (J2000.0)	Binary?	ACIS Brightness	ACIS Variability	HRC Brightness	HRC Variability
B Stars							
159	7 58 50.55	−60 49 28.4	No	Bright	None	Bright	QL
114	7 58 22.26	−60 51 28.0	No	Moderate	None	Bright	None
44	7 57 47.77	−60 36 34.3	No	Off-chip		Moderate	None
3	7 56 46.36	−60 48 58.6	No	Bright	None	Bright	None
181	7 59 21.31	−60 48 56.6	No	Bright	None	Moderate	QL
33	7 57 37.64	−60 54 32.1	No	Off-chip		Moderate	None
185	7 59 27.52	−60 47 46.9	No	Bright	None	Moderate	None
158	7 58 50.26	−60 38 38.1	No	Off-chip		Bright	Stochastic
124	7 58 30.15	−60 41 49.9	No	Moderate	Stochastic	Moderate	None
A Stars							
13	7 57 19.69	−60 48 46.7	No	Faint		Moderate	None
163	7 58 53.12	−60 36 11.2	Yes	Off-chip		Bright	Stochastic
66	7 57 57.33	−60 44 16.4	Yes	Faint		Moderate	None
94	7 58 10.45	−60 51 57.8	No	Moderate	None	Bright	None
131	7 58 32.02	−60 53 51.7	No	Faint		Moderate	None
128	7 58 30.89	−60 37 47.1	Yes	Faint		Moderate	None
29	7 57 31.60	−60 59 30.5	No	CCD=s3		Bright	Stochastic
5	7 56 47.55	−60 56 48.9	Yes	Bright	None	Bright	None
42	7 57 46.09	−60 48 39.2	No	Faint		Bright	Flare
F Stars							
1	7 56 22.50	−60 51 42.2	Yes	Bright	None	Bright	Stochastic
16	7 57 23.18	−60 49 38.4	Yes	Faint		Moderate	None
106	7 58 18.00	−60 45 15.5	Yes	Moderate	None	Moderate	None
10	7 57 16.42	−60 47 12.8	No	Faint		Moderate	Stochastic
92	7 58 08.82	−60 44 40.4	No	Moderate	None	Moderate	None
149	7 58 40.00	−60 41 42.7	No	Faint		Moderate	None
182	7 59 21.32	−60 46 02.6	No	Bright	None	Moderate	None
119	7 58 23.54	−60 37 21.0	No	Bright	None	Moderate	None
108	7 58 19.83	−60 41 58.2	No	Bright	None	Moderate	None
143	7 58 36.44	−60 50 18.3	Yes	Faint		Moderate	None
61	7 57 55.57	−60 40 39.9	No	Faint		Moderate	None
76	7 58 02.36	−60 46 47.6	Yes	Bright	Stochastic	Bright	None
183	7 59 22.08	−60 45 26.7	No	Bright	None	Moderate	None
G Stars							
162	7 58 52.31	−60 53 38.2	Yes	Faint		Moderate	None
65	7 57 56.82	−60 50 34.5	No	Faint		Moderate	None
9	7 57 14.13	−60 40 52.6	Yes	Off-chip		Bright	None
17	7 57 25.11	−60 46 47.8	No	Faint		Moderate	None
71	7 57 59.26	−60 56 54.0	Yes	Faint		Bright	Stochastic
137	7 58 33.36	−60 44 27.5	Yes	Faint		Moderate	Stochastic
140	7 58 35.68	−60 46 52.6	No	Bright	QL	Bright	QL
154	7 58 43.71	−60 32 58.6	Yes	Off-chip		Bright	Stochastic
60	7 57 55.36	−60 48 27.5	Yes	Bright	QL	Bright	None
24	7 57 29.40	−60 50 12.3	Yes	Faint		Moderate	None
152	7 58 43.26	−60 55 26.5	No	Bright	None	Bright	Stochastic
27	7 57 30.88	−60 48 32.2	No	Bright	Flare	Moderate	None
2	7 56 34.56	−60 48 03.6	Yes	Off-chip		Bright	None
186	7 59 32.05	−60 48 45.1	Yes	Bright	Stochastic	Bright	None
156	7 58 48.06	−60 54 14.8	No	Bright	Stochastic	Bright	Stochastic
67	7 57 57.62	−60 53 39.5	No	Bright	None	Moderate	Stochastic
K Stars							
115	7 58 22.89	−60 40 20.5	No	Bright	None	Bright	QL only
161	7 58 51.78	−60 35 20.9	No	Off-chip		Bright	Stochastic
129	7 58 31.52	−60 53 10.6	No	Faint		Moderate	QL
167	7 58 57.55	−60 43 00.9	No	Bright	None	Bright	None

TABLE 1—*Continued*

Paper II Source Number	R.A. (J2000.0)	Decl. (J2000.0)	Binary?	ACIS Brightness	ACIS Variability	HRC Brightness	HRC Variability
132	7 58 32.16	−60 46 01.0	No	Bright	QL	Moderate	None
116	7 58 23.39	−60 54 57.4	Yes	Bright	None	Bright	None
166	7 58 57.21	−60 36 09.9	No	Faint		Moderate	None
14	7 57 20.75	−60 44 03.4	No	Faint		Moderate	None
188	7 59 39.92	−60 42 30.2	Yes	Faint		Moderate	None
107	7 58 19.26	−60 52 00.6	No	Faint		Moderate	None
6	7 56 48.08	−60 46 32.3	Yes	Off-chip		Moderate	None
34	7 57 39.79	−60 46 39.6	Yes	Faint		Moderate	QL
4	7 56 46.88	−60 43 23.2	No	Off-chip		Moderate	Stochastic
72	7 58 00.27	−60 52 12.7	Yes	Bright	Stochastic	Moderate	None
123	7 58 29.80	−60 49 00.6	Yes	Faint		Moderate	None
178	7 59 15.81	−60 47 34.7	Yes	Faint		Moderate	None
165	7 58 56.37	−60 47 22.9	No	Faint		Moderate	None
175	7 59 08.59	−60 50 49.9	No	Faint		Moderate	Stochastic
164	7 58 53.80	−60 54 24.3	Yes	Faint		Moderate	None
202	7 58 56.67	−60 52 16.2	Yes	Faint		Moderate	None
169	7 58 57.60	−60 40 58.5	No	Faint		Moderate	Flare
			M Stars				
180	7 59 17.86	−60 45 18.6	Yes	Faint		Moderate	None
101	7 58 16.55	−60 52 12.7	No	Faint		Moderate	Stochastic
141	7 58 36.08	−60 46 18.2	No	Bright	Flare	Faint	
134	7 58 32.97	−60 51 29.3	Yes	Faint		Moderate	None
170	7 59 00.55	−60 44 10.5	Yes	Faint		Bright	Flare
			Nonmembers				
46	7 57 48.58	−60 31 32.2	No	Off-chip		Moderate	Stochastic
184	7 59 23.18	−60 47 32.2	No	Bright	None	Moderate	None
73	7 58 00.37	−60 40 43.4	No	Faint		Moderate	None
39	7 57 44.02	−60 47 28.2	No	Moderate	None	Moderate	None
19	7 57 24.19	−60 39 49.1	No	Off-chip		Moderate	None
187	7 59 36.43	−60 44 31.8	Yes	Bright	None	Bright	None
8	7 57 11.72	−60 33 09.5	No	Off-chip		Moderate	Stochastic
189	7 59 51.24	−60 43 20.0	No	Off-chip		Bright	QL
12	7 57 19.34	−60 56 27.9	Yes	CCD=s3		Bright	Stochastic
105	7 58 17.81	−60 50 41.7	No	Bright	Flare	Faint	
153	7 58 43.25	−60 41 45.9	No	Faint		Moderate	None
88	7 58 06.11	−60 35 53.8	No	Bright	Stochastic	Bright	None
7	7 56 59.49	−60 49 57.4	Yes	Faint		Moderate	None
31	7 57 36.04	−60 50 26.2	No	Off-chip		Moderate	None
70	7 57 58.29	−60 52 49.0	No	Faint		Moderate	None
151	7 58 42.06	−60 50 40.4	Yes	Faint		Moderate	None
59	7 57 54.71	−60 35 57.7	No	Off-chip		Moderate	Stochastic
173	7 59 05.01	−60 44 27.9	No	Bright	QL	Faint	
			No Counterpart				
11	7 57 18.40	−60 48 16.3	...	Faint		Moderate	Stochastic
18	7 57 25.24	−60 44 59.5	...	Moderate	None	Moderate	QL only
21	7 57 26.73	−60 39 46.9	...	Off-chip		Moderate	Stochastic
25	7 57 29.37	−60 52 11.1	...	Bright	Stochastic	Moderate	None
30	7 57 32.52	−60 41 11.7	...	Faint		Moderate	None
99	7 58 14.38	−60 36 01.1	...	Off-chip		Moderate	None
157	7 58 49.36	−60 42 12.7	...	Moderate	None	Moderate	Stochastic
168	7 58 57.66	−60 43 13.3	...	Faint		Moderate	None
172	7 59 03.85	−60 52 36.9	...	Faint		Moderate	Stochastic
177	7 59 11.74	−60 42 21.6	...	Bright	None	Moderate	None
179	7 59 17.89	−60 55 26.9	...	Off-chip		Bright	Flare
205	7 59 41.17	−60 45 24.1	...	Faint		Moderate	None

Note.—Units of right ascension are hours, minutes, and seconds, and units of declination are degrees, arcminutes, and arcseconds.

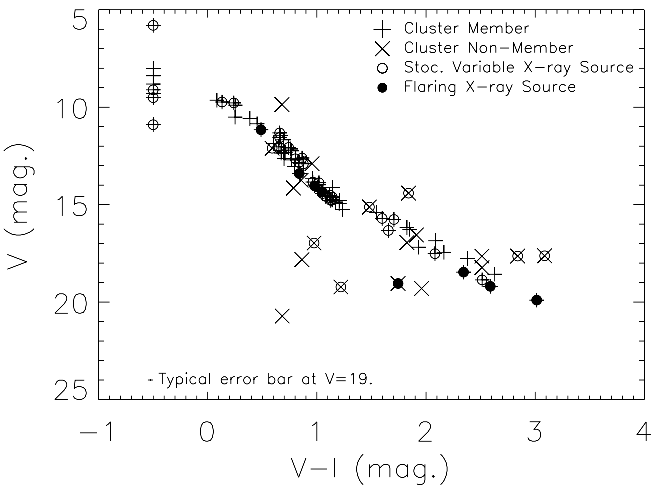

FIG. 2.—Color-magnitude diagram for all optically detected sources in the study. Plus signs indicate cluster members; crosses indicates noncluster members. Open circles show X-ray variables, and filled circles show X-ray flares. The group of sources at $V-I = -0.5$ are B stars with no $V-I$ measurement in Jeffries et al. (2001). Stars that are seen as both flares and variable are noted as flares (*filled circles*) in this plot. The maximum photometric error is shown in the lower left.

being a nonfactor, as there are three HRC observations to compare and only two for ACIS. Hence, the 29 cluster members detected with ACIS represent only 17% of the compared flux levels. So, not only is there is no evidence that HRC saw more changes because of the longer duration between visits, the evidence is that more quiescent level changes are seen on the shorter timescale. The timescale for quiescent level changes is $\leq$14 hr.

It is perhaps possible that only a small group of stars actually change their flux. However, this does not seem to be the case, since only one source showed quiescent level changes among both the HRC and ACIS intervals. One can test for extreme flux variations by comparing the ACIS and HRC flux categories. Since a "faint" source is defined as less than 25 counts, a faint ACIS source is brighter than a faint HRC source. Of the 174 stars in common among the ACIS and HRC observations, only two faint HRC sources were detected as bright in ACIS without the benefit of a flare in one of the observations. Only one of the two is a cluster member, and in this case the quiescent level shift was detected between the two ACIS exposures. No faint ACIS source was detected at more than 2 counts ks^{-1} by the HRC. Thus, order of magnitude shifts in the X-ray quiescent level seem rare.

Two of the 28 HRC observed nonmember or optically unidentified X-ray sources showed a change in their quiescent flux level. One of the 10 such ACIS sources showed a significant change in mean flux. In addition, one nonmember (source 105) that was an ACIS source with more than 2 counts ks^{-1} had less than 25 counts during the 56 ks total HRC observing time. This source seems to have been coming down from a flare state in the very beginning of the first ACIS observation. Thus, this is probably not a case of a change in the quiescent level but the detection of the end of a long-duration flare.

5.2. *Flares*

Each light curve was quantitatively tested for 5 σ flares, as well as for variability relative to the expectations of a constant source. The cumulative findings are summarized in Tables 2 and 3. These tables compare the flare and stochastic variability rates for cluster members and nonmembers, separately for ACIS and HRC. Stochastic variability is common, seen in about one-third of all X-ray sources. The second column of these tables, "obstime," is the summed observation time for all sources of a given type. The idea behind summing the observation time is to gauge how long one would have to observe a single source to detect a flare or other variability. Over the HRC data set four flares were seen at an average of one flare per 1.4 Ms. Among cluster members, a flare was seen once per 1.5 Ms and one flare was seen in 1.1 Ms spent observing other sources. The ACIS data also found flares were more frequent among noncluster sources, but the frequency was higher for both than the HRC data. This is due to the higher ACIS effective area, which eases detection of X-ray sources as well as detection of their variability. One flare was detected in an integrated 478.5 ks of observing time on cluster members, while the noncluster members showed one flare in 165 ks of integrated observing time. The data indicate that the bulk of the variability seen among the cluster members is not large-scale flaring, but stochastic variability—real but small variations that average out over time. We cannot distinguish stochastic variability from the superposition of several small microflares.

5.3. *Bulk Properties*

The fact that ACIS and HRC were used for vastly different time durations makes comparative analysis difficult because the K-S test is sensitive to the total number of photons seen. To help compensate for this, we separately analyzed a subgroup of bright stars. The bright stars (>2 counts ks^{-1}) make up a flux-limited sample. With this more tightly defined sample, HRC observed cluster members showed the same stochastic variability rate (within one) as other objects. During the short ACIS observations, the variability rate noted for bright cluster members was two-thirds that noted for HRC. This is possibly related to the fact that the ACIS observations were 30% of the duration of the HRC exposures. Stochastic variability among noncluster members was slightly higher than 50%.

The similarity of the cluster stars to the field is not too surprising. Foreground (and background) stars are mostly expected to be active (dK–dM) stars, which are well-known flaring variables. NGC 2516 is also relatively close to the Gould Belt, which is populated by young (ZAMS) stars. Bright background X-ray sources are perhaps AGNs, often showing irregular variability. There were only nine bright X-ray sources that were not cluster members; six were found to be variable in one form or another. The existence of an optical counterpart seemed to have no bearing. Two nonmembers (one, either a K star or perhaps a background galaxy and another with no optical counterpart) sustained large changes in quiescent flux, interpretable as flares.

It appears that the low-luminosity ZAMS stars which make up the bulk of the cluster are, if at all different, less variable than stars which are not cluster members, especially when compared to sources with no optical counterparts. There are not enough bright noncluster members to compare with the flux-limited sample. However, support for this conclusion is found in the two flares seen among noncluster members. For the noncluster members, it required an average of 642.5 ks of integrated observing time to detect a flare. Although not statistically significant (due to small numbers), this is less than

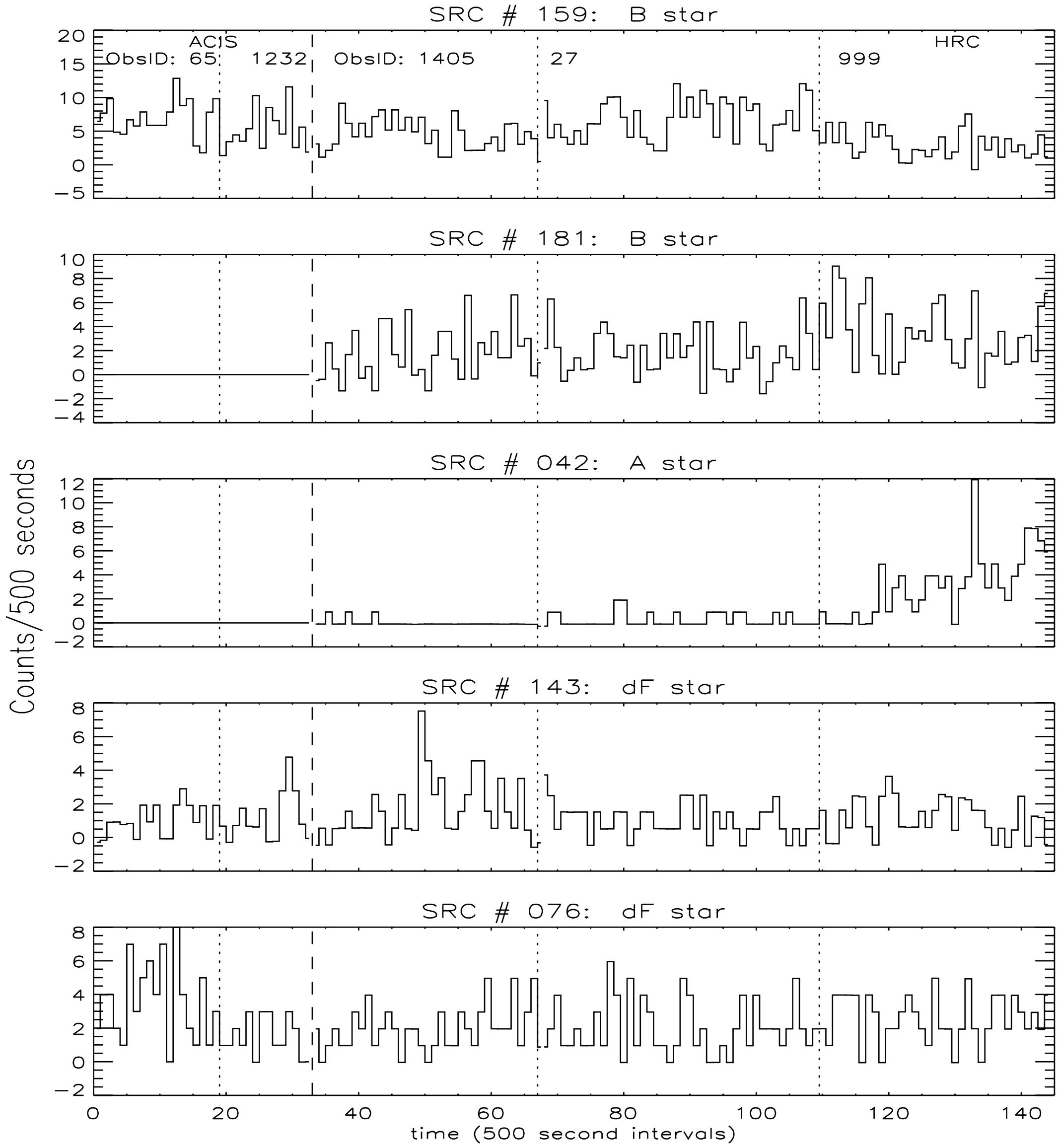

FIG. 3.—Examples of variable light curves. Each of the above light curves is 72.5 ks from start to finish. Vertical dashed lines indicate a change of detector from ACIS-I (*left*) to HRC (*right*). Vertical dotted lines indicate separate observations made with each detector. ObsIDs are indicated at the top of the figure. Src 42, a chemically peculiar A star that only showed significant flux in the later stages of the last observation, was detected as a flare. Spectral types of other sources are indicated. Light curves for sources 181 and 42 have a data gap for the first part because the objects were outside the ACIS field of view during those intervals.

half than the average observing time (1.3 Ms) required to see a flare among the cluster members.

5.4. *Variability as a Function of Spectral Type.*

In Table 4, we compare the stochastic variability of the high-mass stars with that of the low-mass stars. We also compare the results of the "bright" stars against those for "moderate" stars. We find that late-type stars are more than twice as likely to be found stochastically variable than early-type stars. Stochastic variability is also almost twice as common among bright sources as moderate sources.

In Figure 8, we have plotted spectral color versus mean X-ray activity (again taken from Table 4 of Paper II). X-ray activity is certainly a factor in our ability to detect variability. Seventy-five percent (18/24) of the stars with over 2×10^{-5} counts s^{-1} cm^{-2} are found to be variable. Only 56% of the stars with $(1–2) \times 10^{-5}$ counts s^{-1} cm^{-2} are seen to be variable. The fraction of detected variables falls by a factor of more than 2, to 26% if only those stars in the range $(5–10) \times 10^{-6}$counts s^{-1} cm^{-2} are considered. This pattern does not hold for flaring. Flaring is only seen in sources with fluxes *below* 3×10^{-5} counts s^{-1} cm^{-2}.

It is possible that this is indicative of a relationship between stochastic variability and activity. For the cluster members, the ratio of the relative luminosities and the absolute luminosities are the same. Cluster members with lower flux are less X-ray active. However, we are dealing with a very limited number of relatively low flux stars. We do not think this limited data can be used to support this conclusion. Instead, we interpret this result to mean that we are about twice as sensitive to stochastic variability among the bright stars as the moderate stars. This is consistent with the results of our simulations.

To further evaluate this hypothesis, we need to compare sources with similar flux levels. In the flux-limited HRC sample, between 40% and 60% of member stars in each spectral type are detected as variable (if K and M spectral types

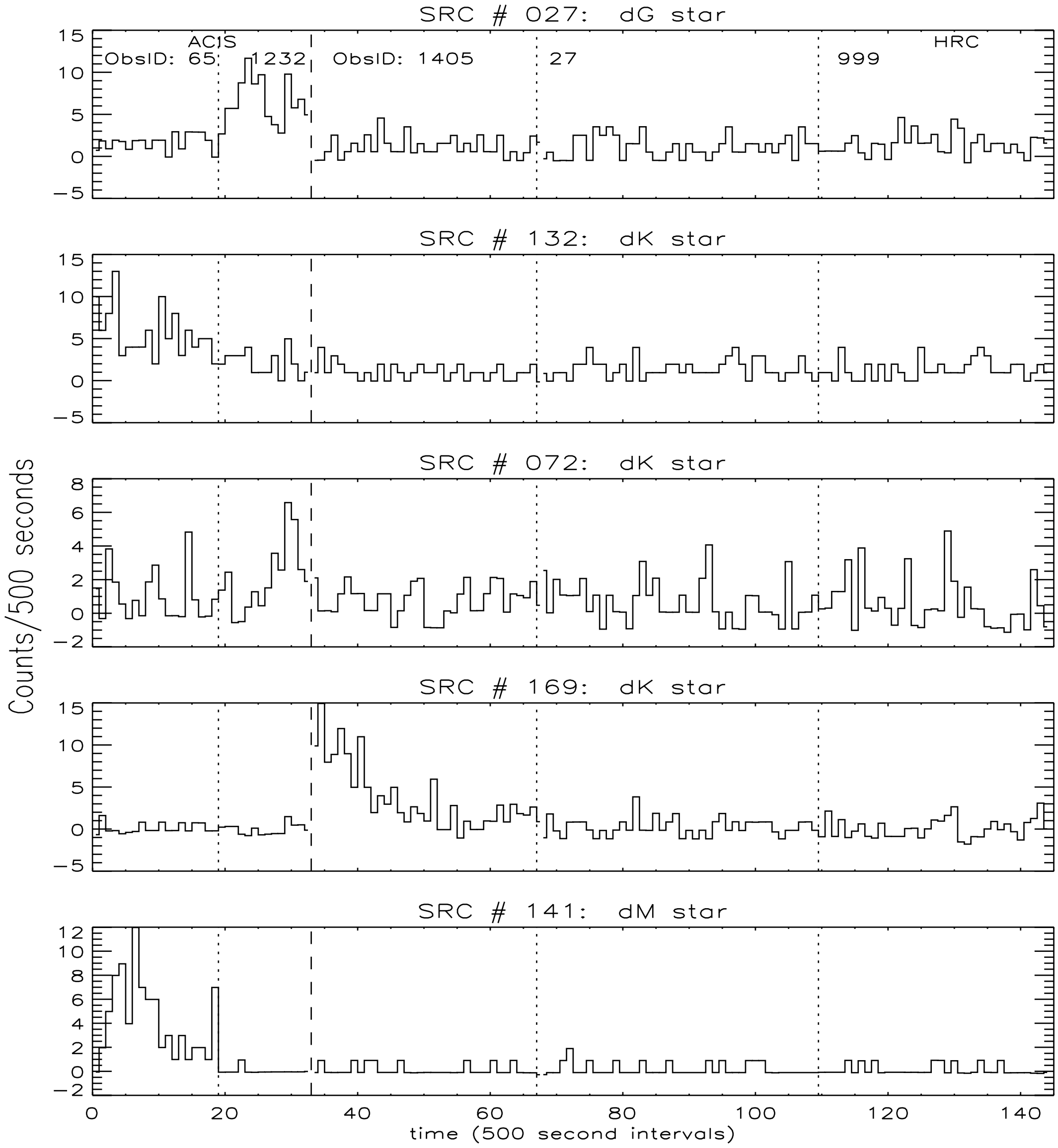

Fig. 4.—These plots are similar to those in Fig. 3. They show, from top to bottom, a dG star, three dK stars, and a dM star. All show the bulk of their flux during a single observing window. All except Src 132 are considered flares. Src 132 was detected as a shift in the quiescent level—the sharp peak in the beginning of the Src 132 observation is too short to be considered a flare.

are combined). Stochastic variability among G, K, and M stars is almost identical in either the HRC or ACIS observation.

In contrast, there is a much lower stochastic variability rate observed among the bright ACIS for B, A, and F stars than for early-type stars observed with HRC. This indicates that the detection of stochastic variability via the K-S test is a function of duration for early-type stars but not a function of the duration of observation for late-type stars. This may indicate that early-type stars vary on longer timescales than late-type stars. Thus, the source of the variability and the X-rays themselves may be different. We can test for duration sensitivity by examining only the 26 bright cluster members observed during ObsID 999 or 1405, along with the combined ACIS observation. Since each of the individual HRC observations is approximately the length of the combined ACIS observations, this gives us a large, flux-limited sample of bright stars observed for approximately the same amount of observing time.

Table 5 shows the results of the analysis. By separating the data by ObsID we obtain a reasonably large (although biased by repeat observations of the same stars) sample of bright stars observed for short amounts of time (17.5–21 ks). The results show that more than 31% of the late-type stars show variability even on short timescales, while less than 22% of the early-type stars show similar variability. This latter number appears to be in the upper end of the range of detection rates, as it is clearly dominated by an anomaly among the A stars in during ObsID 999.

The least variable stars are the B and F stars. Examination of the short-term data sets finds only one bright F star varied stochastically from its mean flux in a short amount of time. When we examine the long duration data in the HRC observations, F stars again have the lowest variability rate, 21%. At the same time, F stars are the brightest X-ray sources in NGC 2516 (Paper II). This ensures that the absence of variability in these stars is intrinsic and not due to low counting statistics.

Overall, the variability seen among the B stars observed by the HRC reflect quiescent level changes in two of the cases.

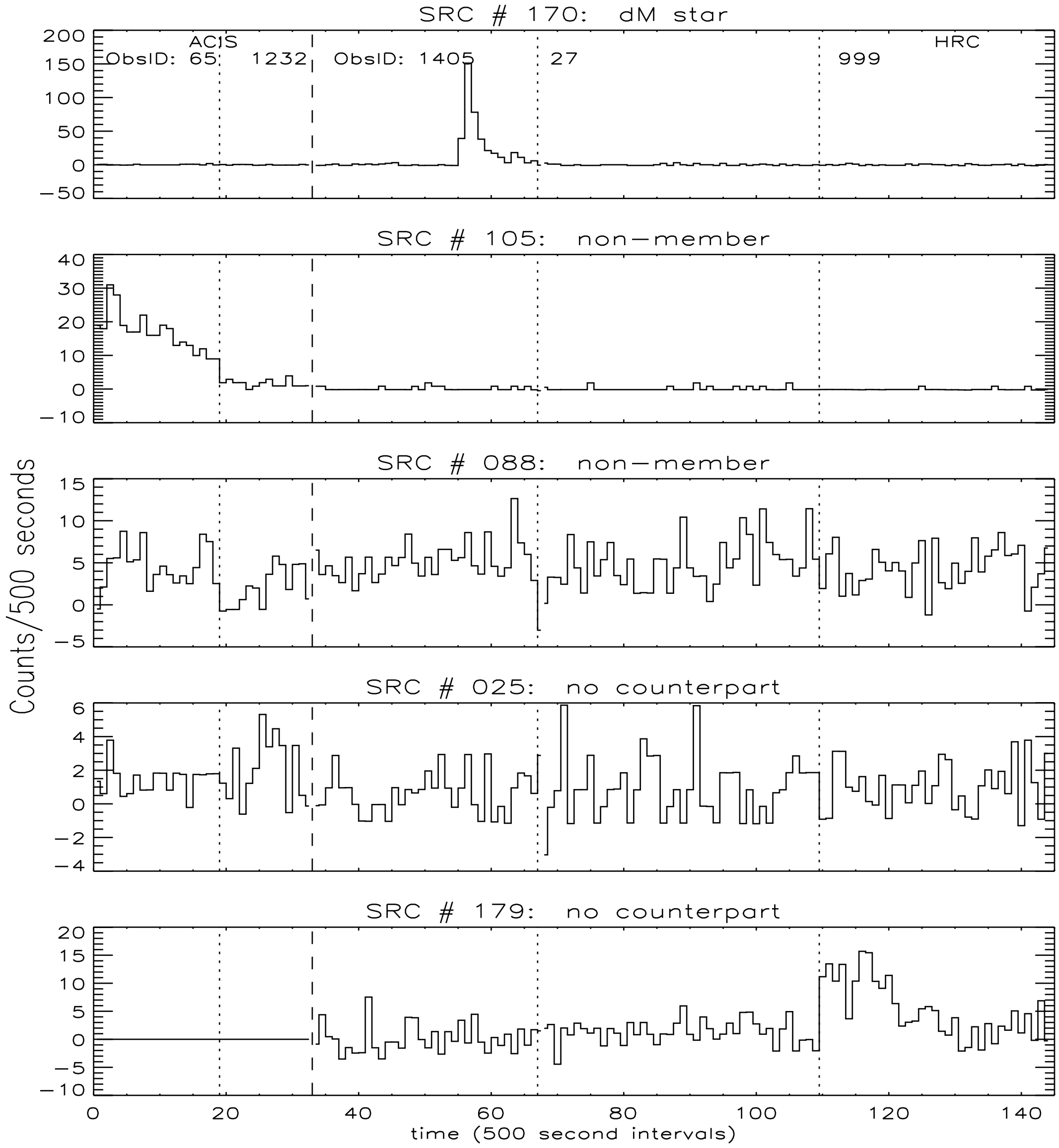

FIG. 5.—Plots are similar to those in Figs. 3 and 4. Src 170, an M star, shows the only observed prototypical flare. Sources 105 and 179 are a nonmember source and a source without an optical counterpart, respectively; they show periods of distinctly higher flux in one observation relative to the others. The remaining sources are shown as examples of stochastic variability.

As with the F stars, only one (of 12 in this case) bright source observed for ≈20 ks showed significant stochastic variability. The fact that these changes are not detected between the two ACIS observations, but are detected in the months separating the HRC observations, weakly suggests that the timescale on which a B star's X-ray luminosity changes is significantly longer than the 14 hr between the ACIS observations.

Similar results are found for the G, K, and M stars. In the case of the temporally and flux-limited sample, the K and M stars are about as variable as G stars to within the statistical errors. Even during the long-duration observations, the bright G stars had about the same variability rate as their later counterparts. The modestly increased detection of X-ray variability among the G stars is probably related to the greater mean X-ray luminosity (Paper II).

The A stars have the most curious results. Ostensibly they should be X-ray–quiet. Yet, as discussed in Paper II, almost all of the chemically peculiar A stars are detected. Further, more than half of them are considered "bright." Variability was detected for five of the 11 A stars observed during short observations. This is a rate similar to the late-type stars. Perhaps this is another indication that the chemical peculiarity is related to the existence of a late-type companion. Alternatively, we note that the bulk of the variable A stars were seen in ObsID 999. We are in a regime with a very low number of stars, and repeated measurements on the same type of stars can vary wildly. This form of "noise" affects not only the conclusions with respect to the A stars, but to each subdivision of X-ray sources.

5.5. *Multiplicity*

In Tables 6 and 7 we assay X-ray variability of cluster members versus multiplicity as determined by the photometric data presented by Jeffries et al. (2001). These include photometric, spectroscopic, and optical binaries, so they are not necessarily short-period binaries. On most counts, the single stars are more active than the binaries. They show more flares and have a far higher variability fraction among the

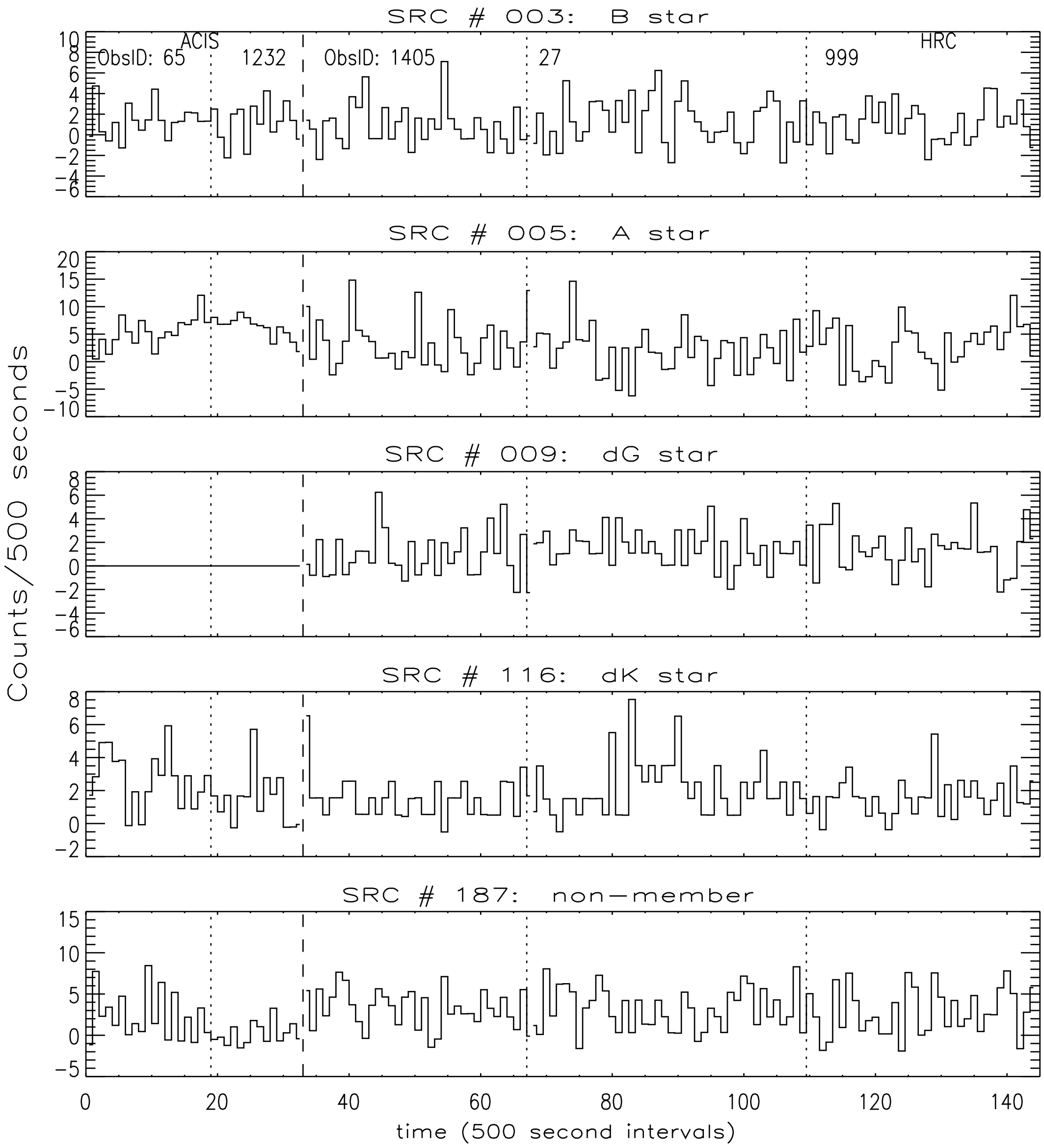

FIG. 6.—Plots are similar to those in Figs. 3, 4, and 5, except that they feature X-ray sources found *not* to deviate from a constant source at over 99% confidence

HRC stars. An obvious explanation is a bias toward detecting variability in single stars over multiples because they vary independently. In this case, the amplitude of the variability in a binary is reduced. On the other hand, if variability is flare-dominated, a binary should flare twice as often as a single star. This latter effect is not seen in our limited data set. In fact, single stars are seen to flare more than binaries.

The small number of X-ray–bright binary stars detected by ACIS leads us to give little weight to the ACIS detection of a fractionally higher rate of variables among the binaries than single cluster members.

5.6. *X-Ray Sources in the Other Three ACIS Observations of NGC 2516*

For the sake of data uniformity and to allow direct statistical comparison, we restricted ourselves to five *Chandra* observations of NGC 2516. We note that ~30 ks of good science data exist in ObsIDs 66, 1229, and 1458. No bright flares were observed in any of the 88 sources detected in an 11.58 ks observation (ObsID =1458). ACIS-S ObsIDs 66 and 1229 detected 63 and 66 sources, respectively. The two combined observations were 22.8 ks in duration. Two flares were observed; this is a rate of 3%, similar to the other observed flare rates. One flare was on a nonmember M star (Src 122), which had less than 25 counts in the HRC and ACIS-I observations and exhibited powerful prototypical flares during the ACIS-S observations. Another M star, this one a cluster member (Src 151), shows a sudden rise in the last 5 ks of ObsID 66.

6. COMPARISON WITH OTHER YOUNG CLUSTERS

The Orion Nebula cluster (ONC) is one of the most well-studied massive young star-forming regions. Much larger and younger than NGC 2516, it is less than 1 million years old with approximately 2000 members. Flaccomio et al. (2003a, 2003b) have analyzed a continuous HRC observation of the ONC. This observation is 63 ks in duration, and it is worthwhile to summarize the results here for comparative purposes. Using similar techniques as those applied to the NGC 2516 data sets, Flaccomio et al. detect about 745 point sources. These sources were examined for variability (Wolk 2003).

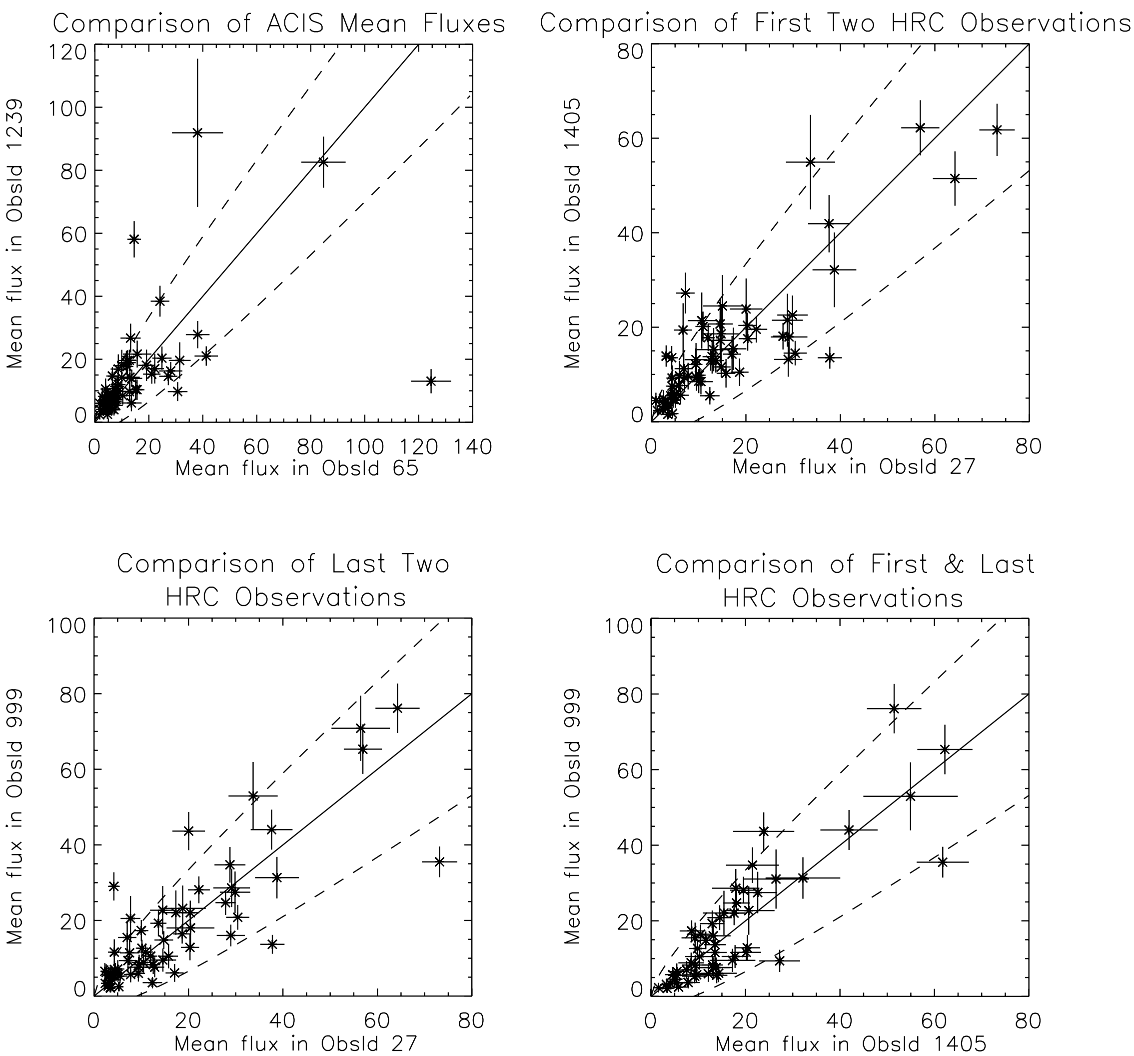

FIG. 7.—Comparison of the observed source fluxes among the five observations studied here. Each source is plotted along with 1 σ errors. The solid lines indicate constant flux, the dashed lines indicate a $\pm 3\sqrt{\text{flux}}$ envelope about the line of constant flux. Most sources have a stable mean flux. All fluxes are in units of 10^{-6} counts s^{-1} cm^{-2}.

TABLE 2

VARIABILITY DURING HRC OBSERVATIONS

	All Sources[a]				X-Ray–bright Only[b]		
Source Type	Number	Obstime[c] (ks)	Stochastic (%)	Flare (%)	Number	Stochastic (%)	Flare (%)
Cluster members:							
B stars	9	504.0	33	0	4	50	0
A stars	9	504.0	22	11	5	40	20
F stars	13	728.0	15	0	2	50	0
G stars	16	896.0	44	0	8	63	0
K stars	21	1176.0	19	4	4	50	0
M stars	4	244.0	25	25	1	0	100
All members	72	4536.0	26	4	24	50	9
Nonmembers	16	448.0	31	0	4	50	0
Unknown ($V > 20$)	12	672.0	33	8	1	0	0
Total	100	5656.0	28	4	29	48	7

NOTE.—Stars listed as "QL only" are not listed as stochastically variable nor flaring.
[a] More than 25 counts.
[b] Brighter than 2 counts ks^{-1}.
[c] Obstime is the sum over all stars of a given type of the individual observing times.

TABLE 3
Variability during ACIS Observations

Members	All Sources[a]				X-Ray–bright Only[b]		
	Number	Obstime[c] (ks)	Stochastic (%)	Flare (%)	Number	Stochastic (%)	Flare (%)
Cluster members:							
B	6	99.0	17	0	4	0	0
A	2	33.0	0	0	1	0	0
F	8	132.0	13	0	6	17	0
G	7	115.5	57	14	7	57	14
K	5	82.5	40	0	5	40	0
M	1	16.5	0	100	1	0	0
Members	29	478.5	28	7	24	33	0
Nonmembers	6	99.0	33	17	5	40	20
Unknown ($V > 20$)	4	66.0	25	0	2	50	0
Total	39	643.5	28	8	31	26	10

[a] More than 25 counts.
[b] Brighter than 2 counts ks^{-1}.
[c] Obstime is the sum over all stars of a given type of the individual observing times.

Using the one-sample K-S test, 22% of stars with over 25 counts are variable at 99% confidence. There are 286 ‘‘bright’’ stars in the HRC/ONC sample with more than 2 counts ks^{-1}. Thirty percent of these (85) are stochastically variable. This latter number is slightly lower than the 27% stochastic variability we report for members of NGC 2516 and much lower than the variability rate reported for the 24 ‘‘bright’’ NGC 2516 stars observed with HRC. True flaring was also rare among the ONC stars. Only 3% have obvious flares as we have defined them here. This is indistinguishable from the 4% flare rate found in NGC 2516. The HRC results in the ONC are consistent with the results of the ACIS studies of the ONC by Feigelson et al. (2002, 2003), who found that found 21.5% of stars with over 50 counts to be variable at 99.5% confidence.

Feigelson et al. also looked for long-term variation between the epochs of their two ONC observations separated by about 6 months. In this category, the results are quite different from NGC 2516. Fully 23% of ONC stars showed quiescent level changes from the mean by more than 3 σ. In NGC 2516, less than 5% of member stars show such changes.

Direct comparison of observations of different clusters is fraught with different effects which are difficult to tease apart. For example, stars less than 1 Myr old tend to be much more X-ray–luminous than ZAMS stars, so even though the NGC 2516 observations are of similar duration to those of the ONC, the latter observations are sensitive to much lower masses and should see flares on much fainter stars. There is a contrast effect that works in the opposite direction. A flare of equal luminosity is easier to see on the fainter ZAMS than on a younger and brighter PMS star. The observations of the ONC were not subject to the variable background level experienced by NGC 2516 measurements. Furthermore, the observation of Orion was shorter than the total useful observing time on NGC 2516. So we cannot argue on the basis of the ONC data alone that the variability rate is lower in the young cluster M42 than the 140 Myr ZAMS cluster NGC 2516.

Two other young clusters observed by *Chandra* have been studied for X-ray variability trends. In their study of NGC 1333, a less massive cluster of similar age to the ONC, Getman et al. (2002) apply a one-sided K-S test to their X-ray

TABLE 4
Stochastic Variability of “Bright” versus “Moderate” Sources

Source Type	“Bright”		“Moderate”	
	Number	Variable (%)	Number	Variable (%)
ACIS Sources				
B–dF	11	9	5	20
dG–dM	13	46	0	. . .
HRC Sources				
B–dF	11	45	21	9
dG–dM	13	46	28	25
Combined ACIS and HRC				
B–dF	22	27	26	11
dG–dM	26	46	28	25

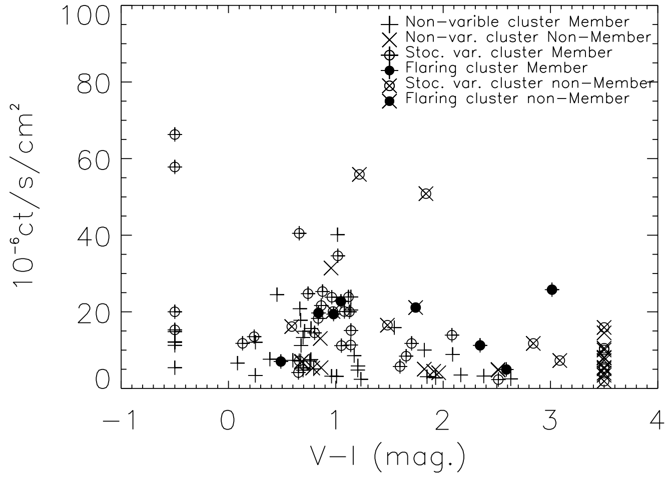

FIG. 8.—Plot of the X-ray activity vs. color for all X-ray sources in this study. Symbols are the same as in Fig. 7. The group of sources at $V-I = -0.5$ are B stars with no $V-I$ measurement in Jeffries et al. (2001). The group of sources at $V-I = 3.5$ were undetected in the Jeffries et al. (2001) optical survey.

light curves. They define a flare as any object with a 99.5% probability of being nonconstant. As with Feigelson et al. (2002, 2003), they do not differentiate between highly impulsive events and stochastic variations. They describe the bulk of the flaring they see as "solar-like" with 1–2 hr rise times and ∼10 hr decay times. They detect stochastic variables ("flares" in their parlance) in 14/77 members (18%) and "possible flares" in an additional 10 (13%) members. However, the bulk of the remaining ∼69% of members were weak. They conclude that about 1/3 of the stars are in each of their three categories: "flaring," "possible flare," and "constant."

A similar cluster is IC 348 (age 1–3 Myr; Herbig 1998; Luhman et al. 1998), which was observed by Preibisch & Zinnecker (2001, 2002) with *Chandra* for 53 ks. They found statistically "significant temporal variability" in about half of the 215 sources detected. This is consistent with the results in NGC 1333 and the ONC for stars that have a 95% probability of being variable. Eighteen of the variables in IC 348 have systematic variability, 11 of which, about 5% of the total, are flares by the definition in § 4.

ZAMS clusters have been well studied by *ROSAT*. The Pleiades have been especially well studied. Specifically, Schmitt et al. (1993) examined the *ROSAT* All Sky Survey data and demonstrated that about 40% of stars showed flux changes of more than a factor of 2. Gagné, Caillault, & Stauffer (1995) confirmed this result and found flares in 12 of 171 sources detected in 50 ks. However, only three of these flares were deviations from the mean by more than 3 σ. Gagné et al. also found that 25% of the stars varied by a factor of 2 on timescales of a year. Micela et al. (1996) found flares in three of 99 stars observed for about 30 ks. They found only three stars had a shift in their mean flux by more than a factor of 2 in observations separated by 6 months. The small number of stars seen to shift their flux on these timescales is similar to that reported here. The published flare rates (>3 σ definition) of 2%–3% are also very similar to the results for the ZAMS NGC 2516.

NGC 2516 has also been observed by *XMM-Newton*. These data have been examined for source variability by Ramsay et al. (2003). They found four sources with significant variability. Three of the four fall within our observed field. Ramsay et al. reported that our SRC 71 (JTP 80), a G star member, was seen to flare. Our SRC 152 (JTP 114), also a G star member, showed a weak impulsive event. SRC 158 (JTP 122), a member B star, had a moderate rise in its flux during one observation. All three of these stars were considered bright and stochastically variable via our analysis.

It is clear that the variability and flare rates are not significantly higher in the younger clusters. For older stars, Marino et al. (2002) found only 10/70 solar-like stars are variable. So, at ages greater than 140 Myr, the situation calms down for stars earlier than K2. The situation is not as clear for the dM stars; Marino et al. (2000) found that almost half of the 65 late-type field stars studied vary.

From these comparisons, we see that the young clusters observed with *Chandra* are all quite similar in terms of their reported stochastic and flaring variability. The only aspect of variability for which younger stars seem different from NGC 2516 is the long-term variability. It is this form of variability the was easiest to study in the *ROSAT* examinations of the Pleiades. While the reported fraction of long-term variables seems high, long-term shifts had been defined in terms of variation by more than a factor of 2; when this is recast as 3 σ deviations, the results for The Pleiades and NGC 2516 are similar. The ONC, on the other hand, does show a significant increase in the fraction of significant quiescent level shifts. This may indicate that the global magnetic field strength around very young stars is much less stable than that of ZAMS stars.

TABLE 5

THE PROBABILITY OF DETECTING ANY VARIABILITY IN A SINGLE SHORT OBSERVATION

	ObsID 1405		ObsID 999		Both HRC		Both ACIS		HRC+ACIS	
Type (1)	Number of Stars (2)	Variable (%) (3)	Number of Stars (4)	Variable (%) (5)	Number of Stars (6)	Variable (%) (7)	Number of Stars (8)	Variable (%) (9)	Number of Stars (10)	Variable (%) 11)
B stars	4	25	4	0	8	13	4	0	12	8
A stars	5	20	5	80	10	50	1	0	11	45
F stars	1	0	2	0	3	0	6	17	9	11
G stars	8	13	8	25	16	19	7	71	23	35
K+M stars	5	40	4	25	9	33	6	50	15	40

NOTE.—Col. (1): Type. Col. (2): Number of bright stars of each spectral type observed during ObsID 1405. Col. (3): Fraction of those found to be variable in a study of data from the single 17 ks observation. Cols. (4) and (5): Same as Cols. (2) and (3), but for the 17.5 ks ObsID 999 observation. Cols. (6) and (7): Sum of the results from the previous two sets of columns. Cols. (8) and (9): Results obtained by studying the light curves of X-ray bright cluster members are placed in the combined 16.5 ks of data from the two ACIS observations. Cols. (10) and (11): Sum of the results from the previous two sets of columns.

TABLE 6
Member Stars Sorted by Photometric Multiplicity—HRC

	Binaries			Single Stars		
Spectral Type	Number	Stochastic (%)	Flare (%)	Number	Stochastic (%)	Flare (%)
B	0	...	...	9	33	0
A	4	25	0	5	20	20
F	5	20	0	8	13	0
G	9	33	0	7	42	0
K	9	11	0	12	33	8
M	3	0	33	1	100	0
Total	30	20	3	42	24	5

However, over the range of the first 140 million years of a star's life, neither flaring, nor stochastic variability, change much.

7. CONCLUSIONS

We have extracted and background-corrected 103 light curves derived from 206 sources contained within the HRC-I observations of NGC 2516. We have calculated meaningful variability properties for these 103 by testing each light curve for variability and flaring and for a shift in the mean flux. Variability was found in about 32% of the X-ray sources. We find that flare-type variability is seen in about 4% of all ZAMS stars during 72.5 ks of observation. Large flare rates seem similar among all X-ray sources in this sample. When comparing the results from NGC 2516 with those of other clusters, it is difficult to compare like sources observed with like detectors. Inhomogeneities in the data set and a dearth of bright sources in all spectral types limit our ability to draw firm conclusions. Taking the data at face value we find the following:

1. ZAMS stars are more stable in their X-ray luminosity than typical background and foreground sources. This result is contained within each of the NGC 2516 observations and the integrated result. Thus, we consider it quite robust.

2. M stars flare somewhat more often than other stars. Again, this result is contained within each NGC 2516 data set, the integrated data set, and is borne out by other observations of other clusters. Flares of the same luminosity are easier to see on dM stars than flares on brighter G and K stars. This is a bias only if the energy contained in a flare is independent of the total energy available to the star.

3. G star members are most prone to being detected as stochastically variable. This could be a result of G stars tending to be the brightest sources and hence the sources for which we have the greatest sensitivity to variability. On the other side of this analysis, ZAMS B and F stars are the most stable in their X-ray luminosity.

4. Change in the quiescent level, or variability on timescales longer than a single observation, is observed in less than 5% of cases. This result is in contrast to the results from Feigelson et al. (2003) for the ONC.

5. The X-ray flux from multiple ZAMS stars tends to be at least as stable as that from single stars. This finding is in contrast to that of Stelzer et al. (2000) for younger stars.

6. The occurrence of short timescale variability is about 30%, which is close to the level observed in the Orion Nebular Cluster.

7. Flare rates are also very similar among the different clusters examined. The *magnitude* of the flares in the older clusters is smaller, but the rate of occurrence of large ($>5\ \sigma$), short-lived, flux increases is quite similar.

The first three points are expected and not highly controversial. The intracluster comparison of the G stars with the earlier members seems robust. This is especially clear in the comparison of the short-term variability of bright stars. The flux of the stars, the number of stars, and the observation time are very similar in this case. The results are strikingly different, with the G stars showing much more variability in the short observations. The discrepancy between early and late stars recurs when comparing only "moderate" sources or only the "bright" sources as shown in Table 4.

TABLE 7
Member Stars Sorted by Photometric Multiplicity—ACIS

	Binaries			Single Stars		
Spectral Type	Number	Stochastic (%)	Flare (%)	Number	Stochastic (%)	Flare (%)
B	0	...	...	6	17	0
A	1	0	0	1	0	0
F	3	33	0	5	0	0
G	2	100	0	5	40	20
K	2	50	0	3	33	0
M	0	...	...	1	0	100
Total	8	50	0	21	19	10

It is in the fourth and fifth points that we begin to see the demarcation between the highly active and rapidly evolving PMS stars and the internal stability that is achieved by the time stars arrive on the ZAMS. However, it needs to be stressed that the fourth and fifth points are not as robust as the first three. Clusters are biased because younger clusters are brighter; hence, some effects, like quiescent level shifts, are easier to see and others, like flaring, may become more difficult to detect.

The last two points strongly indicate that variability and flaring are not strong functions of age. Our ability to detect X-rays, and hence their variations, becomes limited as stars age and their coronal emission lowers. There is no evidence that suggests that the presence of variability in coronal emission changes with age, at least through the ZAMS. Given longer observation intervals it seems probable that all PMS and ZAMS stars will be found to be nonconstant. This would not be surprising given that the 4.6 Gyr old Sun impulsively flares in X-rays and is also periodic on decadal timescales. Our next steps in understanding the variability of stellar X-rays may well need to concentrate on deeper observations. We need to focus on identifying and describing the light-curve morphology and the spectral changes that accompany changes in photon arrival rates.

This project is supported by the *Chandra* X-Ray Center under NASA contract NAS8-39073. PWDetect has been developed by scientists at Osservatorio Astronomico di Palermo G. S. Vaiana thanks to Italian CNAA and MURST (COFIN) grants. We thank the anonymous referee for many helpful comments.

REFERENCES

Dachs, J., & Kabus, H. 1989, A&AS, 78, 25
Damiani, F., Flaccomio, E., Micela, G., Sciortino, S., Harnden, F. R., Jr., Murray, S. S., Wolk, S. J., & Jeffries, R. D. 2003a, ApJ, 588, 1009 (Paper II)
Feigelson, E. D., Broos, P., Gaffney, J. A., III, Garmire, G., Hillenbrand, L. A., Pravdo, S. H., Townsley, L., & Tsuboi, Y. 2002, ApJ, 574, 258
Feigelson, E. D., & Decampli, W. M. 1981, ApJ, 243, L89
Feigelson, E. D., Gaffney, J. A., III, Garmire, G., Hillenbrand, L. A., & Townsley, L. 2003, ApJ, 584, 911
Flaccomio, E., Damiani, F., Micela, G., Sciortino, S., Harnden, F. R., Jr., Murray, S. S., & Wolk, S. J. 2003a, ApJ, 582, 382
———. 2003b, ApJ, 582, 398
Gagné, M., Caillault, J.-P., & Stauffer, J. R. 1995, ApJ, 450, 217
Garcia, H. A. 2000, ApJS, 127, 189
Getman, K. V., Feigelson, E. D., Townsley, L., Bally, J., Lada, C. J., & Reipurth, B. 2002, ApJ, 575, 354
Harnden, F. R., Jr., et al. 2001, ApJ, 547, L141 (Paper I)
Herbig, G. H. 1998, ApJ, 497, 736
Jeffries, R. D., Thurston, M. R., & Hambly, N. C. 2001, A&A, 375, 863
Jeffries, R. D., Thurston, M. R., & Pye, J. P. 1997, MNRAS, 287, 350
Luhman, K. L., Rieke, G. H., Lada, C. J., & Lada, E. A. 1998, ApJ, 508, 347
Marino, A., Micela, G., & Peres, G. 2000, A&A, 353, 177
Marino, A., Micela, G., Peres, G., & Sciortino, S. 2002, A&A, 383, 210
Meynet, G. Mermilliod, J.-C., & Maeder, A. 1993, A&AS, 98, 477
Micela, G., Sciortino, S., Kashyap, V., Harnden, F. R., Jr., & Rosner, R. 1996, ApJS, 102, 75
Montmerle, T., Koch-Miramond, L., Falgarone, E., & Grindlay, J. E. 1983, ApJ, 269, 182
Preibisch, T., & Zinnecker, H. 2001, AJ, 122, 866
———. 2002, AJ, 123, 1613
Ramsay, G., Harra, L., & Kay, H. 2003, MNRAS, 341, 1388
Schmitt, J. H. M. M., Kahabka, P., Stauffer, J., & Piters, A. J. M. 1993, A&A, 277, 114
Sciortino, S., et al. 2001, A&A, 365, L259
Stelzer, B., Neuhäuser, R., & Hambaryan, V. 2000, A&A, 356, 949
Wolk, S. J. 2003, in Proc. 12th Cambridge Workshop on Cool Stars, Stellar Systems, and The Sun, ed. A. Brown, G. M. Harper, & T. R. Ayres (Boulder: Univ. Colorado), 81